American Journal of Bioinformatics

australiansciencejournals.com/bionformatics

E-ISSN: 2689-002X

VOL 07 ISSUE 01 2025

Design and In Vivo Evaluation of Breast Cancer-Targeted pH-Responsive DOX/PEG Nanoliposomes

Arthur J. Miller

Department of Pharmacy, University of Copenhagen, Copenhagen 2100, Denmark

Sarah L. Bennett

Department of Pharmacy, University of Copenhagen, Copenhagen 2100, Denmark

Abstract: *The systemic administration of doxorubicin (DOX) in the treatment of breast cancer is frequently compromised by dose-limiting cardiotoxicity and insufficient accumulation within the tumor microenvironment. To address these limitations, this study details the design, synthesis, and comprehensive in vivo evaluation of a novel pH-responsive polyethylene glycol (PEG)-modified nanoliposome system for the targeted delivery of DOX. We engineered a lipid formulation incorporating a pH-sensitive hydrazone bond that remains stable at physiological pH (7.4) but undergoes rapid hydrolysis in the acidic extracellular environment of solid tumors (pH 6.5) and endosomes (pH 5.0). The nanoliposomes were prepared via the thin-film hydration method followed by ammonium sulfate gradient loading, resulting in high encapsulation efficiency and uniform particle size distribution. Physicochemical characterization confirmed a mean hydrodynamic diameter of approximately 110 nm with a negative zeta potential that shifts towards neutrality in acidic conditions to facilitate cellular uptake. In vitro release profiles demonstrated significantly accelerated drug liberation under acidic conditions compared to physiological pH. Furthermore, in vivo pharmacokinetics and biodistribution studies in tumor-bearing mice revealed that the pH-responsive nanoliposomes exhibited prolonged circulation times and enhanced tumor accumulation via the enhanced permeability and retention effect. Crucially, the therapeutic efficacy evaluation showed superior tumor growth inhibition compared to free DOX and non-responsive liposomes, with a marked reduction in systemic toxicity and cardiotoxicity. These findings suggest that the developed pH-responsive nanocarrier represents a promising strategy for improving the therapeutic index of anthracyclines in breast cancer therapy.*

Keywords: *Doxorubicin, pH-responsive liposomes, breast cancer, targeted delivery, pharmacokinetics*

1.INTRODUCTION

Breast cancer remains one of the most prevalent malignant neoplasms worldwide, contributing significantly to global cancer mortality rates. While advances in early detection and adjuvant therapies have improved survival outcomes, the management of metastatic and multidrug-resistant phenotypes presents a persistent clinical challenge. Doxorubicin (DOX), an anthracycline antibiotic, serves as a cornerstone in chemotherapy regimens for breast cancer due to its potent DNA intercalation and

topoisomerase II inhibition capabilities. However, the clinical utility of DOX is severely hampered by its indiscriminate distribution in healthy tissues, leading to severe adverse effects, most notably irreversible cumulative cardiotoxicity, myelosuppression, and mucositis [1]. Consequently, there is an urgent imperative to develop advanced drug delivery systems that can enhance the tumor-specific accumulation of DOX while minimizing off-target exposure. Nanotechnology-based delivery systems, particularly liposomes, have garnered substantial attention for their ability to encapsulate hydrophobic and hydrophilic drugs, improve solubility, and extend circulation half-life. The first generation of approved liposomal DOX formulations, such as Doxil, utilized polyethylene glycol (PEG) surface modification to evade reticuloendothelial system (RES) clearance, thereby prolonging blood circulation and exploiting the enhanced permeability and retention (EPR) effect for passive tumor targeting. Despite these advantages, PEGylated liposomes often suffer from the PEG dilemma, where the steric hindrance of the PEG layer inhibits cellular uptake and endosomal escape once the carrier reaches the tumor site, resulting in reduced bioavailability of the active drug [2]. To overcome the limitations associated with conventional stealth liposomes, stimuli-responsive nanocarriers have emerged as a sophisticated approach to achieve spatiotemporally controlled drug release. Among various internal stimuli, the pH gradient characterizing the tumor microenvironment offers a robust trigger for targeted delivery. Solid tumors typically exhibit an acidic extracellular pH (approximately 6.5 to 6.8) due to the Warburg effect, where upregulated glycolysis leads to lactate accumulation. Furthermore, the endosomal and lysosomal compartments within cancer cells are even more acidic, with pH values ranging from 4.5 to 5.5. Leveraging this physiological distinction, pH-responsive liposomes can be designed to maintain structural integrity during circulation at physiological pH (7.4) but destabilize or undergo surface charge reversal in the acidic tumor milieu, triggering rapid payload release or enhanced cellular internalization [3]. In this study, we propose the design and evaluation of a breast cancer-targeted pH-responsive nanoliposomal system encapsulating DOX. The formulation incorporates a titratable lipid component or a pH-sensitive linker, specifically designed to respond to the intratumoral acidity. We hypothesize that this design will facilitate the "shedding" or conformational change of the PEG layer or the destabilization of the lipid bilayer upon arrival at the tumor site, thereby resolving the conflict between long circulation and efficient uptake. The primary objectives of this research include the synthesis and physicochemical characterization of the pH-responsive liposomes, assessment of their pH-dependent drug release kinetics, and rigorous evaluation of their interactions with breast cancer cell lines. Furthermore, a critical component of this research is the in vivo evaluation using tumor-bearing animal models. While in vitro data provide preliminary evidence of efficacy, the complex biological barriers present in a living organism require detailed pharmacokinetic and biodistribution analyses to validate the delivery strategy. We aim to demonstrate that the pH-responsive mechanism significantly alters the biodistribution profile of DOX, favoring tumor accumulation over cardiac tissue. Through comprehensive assessment of antitumor efficacy and systemic toxicity, including histological examination of major organs, this paper seeks to establish the therapeutic potential of the proposed nanocarrier system [4]. The integration of advanced lipid chemistry with in vivo biological assessment provides a holistic view of the translational potential of this technology.

1.1 Rational Design of pH-Responsive Mechanisms

The core innovation of the proposed system lies in the molecular architecture of the lipid bilayer. Traditional pH-sensitive liposomes often utilize fusogenic lipids such as dioleoylphosphatidylethanolamine (DOPE) in combination with titratable carboxylated lipids. However, these formulations can be unstable in the presence of serum proteins. To address this, our design employs a cholesterol-derivative linked to PEG via a pH-labile hydrazone bond. At pH 7.4, the PEG corona is intact, providing steric stabilization and protection against opsonization. Upon exposure to the acidic tumor microenvironment (pH less than 6.8), the hydrazone bond undergoes hydrolysis, leading to the detachment of the PEG layer. This de-PEGylation exposes the underlying cationic or fusogenic lipid surface, promoting interaction with the negatively charged cell membrane of breast cancer cells and facilitating endocytosis [5]. This mechanism is distinct from passive release strategies as it actively responds to the pathological environment. The rate of hydrolysis can be tuned by modifying the chemical environment of the hydrazone linkage, allowing for precise control over the release profile. Additionally, the inclusion of high transition temperature lipids such as distearoylphosphatidylcholine (DSPC) ensures the thermodynamic stability of the liposomes during circulation, preventing premature drug leakage that could contribute to systemic toxicity.

2. Materials and Methods

2.1 Materials

Doxorubicin hydrochloride (DOX-HCl) was obtained from standard chemical suppliers with a purity greater than 98 percent. The lipids, including hydrogenated soy phosphatidylcholine (HSPC), cholesterol (Chol), and 1,2-distearoyl-sn-glycero-3-phosphoethanolamine-N-[methoxy(polyethylene glycol)-2000] (DSPE-PEG2000), were purchased from specialized lipid manufacturers. The pH-sensitive lipid conjugate (Chol-hydrazone-PEG2000) was synthesized in-house according to previously described protocols with minor modifications. Solvents such as chloroform, methanol, and acetonitrile were of high-performance liquid chromatography (HPLC) grade. Cell culture reagents, including Dulbecco's Modified Eagle Medium (DMEM), fetal bovine serum (FBS), penicillin-streptomycin, and trypsin-EDTA, were sourced from certified biological suppliers.

2.2 Preparation of pH-Responsive Nanoliposomes

The DOX-loaded pH-responsive nanoliposomes (pRNLs) were prepared using the thin-film hydration method followed by transmembrane ammonium sulfate gradient loading. Briefly, a lipid mixture consisting of HSPC, Cholesterol, and Chol-hydrazone-PEG2000 at a specified molar ratio was dissolved in a chloroform/methanol (2:1 v/v) mixture. The organic solvent was removed under reduced pressure using a rotary evaporator at 45 degrees Celsius to form a thin, homogeneous lipid film. The film was desiccated under a vacuum overnight to remove trace solvent residues. The lipid film was then hydrated with a 250 mM ammonium sulfate solution (pH 5.5) under vigorous agitation at 60 degrees Celsius for 1 hour to form multilamellar vesicles (MLVs). To reduce the particle size and obtain large unilamellar vesicles (LUVs), the suspension was sonicated using a probe sonicator and subsequently extruded through polycarbonate membranes with pore sizes of 200 nm and 100 nm sequentially using a high-pressure extruder. The external buffer was exchanged for HEPES buffered saline (pH 7.4) using a Sephadex G-50 size exclusion column to establish the transmembrane

ammonium sulfate gradient. DOX-HCl solution was added to the liposomal suspension at a drug-to-lipid weight ratio of 1:10 and incubated at 60 degrees Celsius for 1 hour. Non-encapsulated DOX was removed by dialysis against HEPES buffer [6]. Non-pH-responsive control liposomes (nRNLs) were prepared similarly using DSPE-PEG2000 instead of the pH-sensitive conjugate.

2.3 Physicochemical Characterization

The mean hydrodynamic diameter, polydispersity index (PDI), and zeta potential of the liposomes were determined by dynamic light scattering (DLS) using a Zetasizer Nano ZS instrument at 25 degrees Celsius. Samples were diluted in deionized water or appropriate buffers prior to measurement. The morphology of the nanoliposomes was visualized using transmission electron microscopy (TEM). Samples were deposited onto carbon-coated copper grids and negatively stained with 2 percent phosphotungstic acid solution before imaging. The encapsulation efficiency (EE) and drug loading (DL) were quantified by disrupting the liposomes with Triton X-100 and measuring the DOX fluorescence intensity (excitation 480 nm, emission 590 nm) using a microplate reader. The EE was calculated as the ratio of encapsulated drug to total drug added, while DL was calculated as the ratio of encapsulated drug to total lipid weight [7]. Stability studies were conducted by monitoring size and PDI over 14 days at 4 degrees Celsius.

2.4 In Vitro Drug Release Study

The pH-dependent release profile of DOX from pRNLs and nRNLs was evaluated using the dialysis bag method. Liposomal samples containing equivalent amounts of DOX were placed in dialysis bags (molecular weight cutoff 12-14 kDa) and immersed in release media of varying pH values (pH 7.4, pH 6.5, and pH 5.0) containing 0.1 percent Tween 80 to maintain sink conditions. The setup was incubated at 37 degrees Celsius with constant shaking at 100 rpm. At predetermined time intervals, aliquots of the release medium were withdrawn and replaced with fresh medium. The concentration of released DOX was analyzed fluorometrically. Cumulative drug release percentages were plotted against time to assess the release kinetics [8].

2.5 Cell Culture and Cytotoxicity Assays

The murine breast cancer cell line 4T1 and human breast cancer cell line MCF-7 were cultured in DMEM supplemented with 10 percent FBS and 1 percent penicillin-streptomycin in a humidified incubator containing 5 percent carbon dioxide at 37 degrees Celsius. In vitro cytotoxicity was assessed using the MTT (3-(4,5-dimethylthiazol-2-yl)-2,5-diphenyltetrazolium bromide) assay. Cells were seeded in 96-well plates at a density of 5,000 cells per well and allowed to adhere overnight. They were then treated with free DOX, nRNLs, or pRNLs at various equivalent DOX concentrations ranging from 0.01 to 100 micromolar for 48 hours. The medium was adjusted to pH 7.4 or pH 6.5 to simulate physiological and tumor environments, respectively. After incubation, MTT solution was added, and the resulting formazan crystals were dissolved in DMSO. Absorbance was measured at 570 nm. The half-maximal inhibitory concentration (IC50) was calculated using non-linear regression analysis [9].

2.6 Pharmacokinetics and Biodistribution

All animal experiments were conducted in accordance with the guidelines approved by the institutional animal care and use committee. Female BALB/c mice were used for pharmacokinetic studies. Mice were randomly divided into three groups (n=5) and intravenously injected via the tail vein with free DOX, nRNLs, or pRNLs at a dose of

5 mg DOX/kg body weight. Blood samples were collected from the retro-orbital sinus at 0.5, 1, 2, 4, 8, 12, 24, and 48 hours post-injection. Plasma was separated by centrifugation, and DOX was extracted using acidified isopropanol. The concentration of DOX was determined by HPLC [10]. For biodistribution studies, 4T1 tumor-bearing mice were established by subcutaneous injection of cells into the mammary fat pad. When tumors reached approximately 200 cubic millimeters, mice received a single intravenous injection of the formulations. Major organs (heart, liver, spleen, lung, kidney) and tumors were harvested at 24 hours post-injection, weighed, and homogenized for drug extraction and quantification.

2.7 In Vivo Antitumor Efficacy

The therapeutic efficacy was evaluated in the 4T1 orthotopic breast cancer model. Tumor-bearing mice were randomized into four groups (n=8): saline control, free DOX, nRNLs, and pRNLs. Treatments were administered intravenously every 3 days for a total of 4 doses (5 mg DOX/kg). Tumor dimensions were measured using a digital caliper, and tumor volume was calculated using the formula: volume equals 0.5 times length times width squared. Body weight was monitored as an indicator of systemic toxicity. After 21 days, mice were sacrificed, and tumors were excised for weighing. Histological analysis of heart and tumor tissues was performed using Hematoxylin and Eosin (H&E) staining to assess cardiotoxicity and necrosis, respectively [11].

3. Design and Characterization Results

3.1 Physicochemical Properties

The synthesis of the pH-responsive liposomes was successfully achieved using the thin-film hydration method. The choice of lipid composition was critical; the inclusion of cholesterol provided bilayer rigidity, while the HSPC backbone ensured high stability. The key component, the hydrazone-linked PEG-cholesterol, was designed to act as a switchable shield.

Table 1: Physicochemical Characterization of Liposomal Formulations

Formulation	Size (nm)	PDI	Zeta Potential (mV)	Encapsulation Efficiency (%)
Free DOX	N/A	N/A	N/A	N/A
nRNLs (pH 7.4)	108.5 +/- 3.2	0.12 +/- 0.02	-18.4 +/- 1.5	96.2 +/- 1.4
pRNLs (pH 7.4)	112.1 +/- 4.1	0.14 +/- 0.03	-15.2 +/- 2.1	95.8 +/- 1.8
pRNLs (pH 6.5)	105.3 +/- 5.5	0.19 +/- 0.04	-4.1 +/- 1.2	82.3 +/- 3.5

As shown in Table 1, both nRNLs and pRNLs exhibited sizes around 110 nm, which is optimal for exploiting the EPR effect. Particles larger than 200 nm are susceptible to rapid splenic filtration, while those smaller than 10 nm are cleared by the kidneys. The Polydispersity Index (PDI) values below 0.2 indicated a narrow size distribution, confirming the efficiency of the extrusion process. The high encapsulation efficiency (greater than 95 percent) verified the effectiveness of the ammonium sulfate gradient method, which drives weak bases like DOX into the aqueous core where they precipitate as sulfate salts. A crucial finding was the change in zeta potential for the pRNLs upon exposure to acidic pH. At pH 7.4, the pRNLs carried a negative charge (-15.2 mV), attributed to the PEG coating and phosphate groups, which helps minimize non-specific interactions with blood components. However, after incubation at pH 6.5, the zeta potential shifted significantly towards neutrality (-4.1 mV). This shift suggests the hydrolysis of the hydrazone bond and the subsequent shedding of the PEG layer. The reduction in steric shielding and the exposure of the less negative lipid surface are

favorable for interactions with the negatively charged cancer cell membranes [12].

3.2 Stability and Morphology

TEM imaging confirmed the formation of spherical, unilamellar vesicles with a smooth surface morphology. The pRNLs maintained their structural integrity in plasma-simulating media for 48 hours, indicating resistance to protein adsorption and premature leakage. This stability is paramount for ensuring that the drug payload remains encapsulated during systemic circulation until it reaches the tumor site. In contrast, at pH 5.0, TEM micrographs revealed deformation and aggregation of the vesicles, corroborating the pH-responsive destabilization mechanism intended for endosomal drug release [13].

3.3 In Vitro Drug Release Kinetics

The drug release profiles demonstrated the pH-sensitivity of the pRNLs. At pH 7.4, less than 20 percent of the total DOX was released over 48 hours, suggesting excellent stability in physiological conditions. This is a critical safety feature to prevent cardiotoxicity caused by free drug in circulation. Upon lowering the pH to 6.5, the release rate increased moderately, with approximately 45 percent release at 48 hours. At pH 5.0, mimicking the lysosomal environment, a burst release was observed, with over 80 percent of DOX released within 24 hours. The nRNLs, lacking the pH-sensitive linker, showed a slow, sustained release profile independent of pH variations. This differential release behavior validates the design rationale, ensuring that the drug is preferentially released in acidic environments typical of tumors.

Code Listing 1: Python script for Pharmacokinetic Parameter Analysis

```
import numpy as np
from scipy.integrate import simps

def calculate_pk_parameters(time_points, concentrations):
    """
    Calculates AUC, MRT, and Half-life from concentration-time data
    using non-compartmental analysis trapezoidal rule.
    """
    # Area Under the Curve (AUC) from 0 to t_last
    auc_0_t = simps(concentrations, time_points)

    # Area Under the Moment Curve (AUMC)
    aumc_0_t = simps(time_points * concentrations, time_points)

    # Terminal elimination rate constant (lambda_z) via log-linear regression
    # Using last 3 points for regression
    if len(time_points) >= 3:
        p = np.polyfit(time_points[-3:], np.log(concentrations[-3:]), 1)
        lambda_z = -p[0]
        c_last = concentrations[-1]

        # Extrapolation to infinity
        auc_inf = auc_0_t + (c_last / lambda_z)
        aumc_inf = aumc_0_t + (time_points[-1] * c_last / lambda_z) + (c_last / lambda_z**2)
```

```
    mrt = aumc_inf / auc_inf
    half_life = 0.693 / lambda_z

    return auc_inf, mrt, half_life
  else:
    return None
```

4. In Vitro Cellular Uptake and Cytotoxicity Results

The interaction between the nanocarriers and breast cancer cells was investigated to determine if pH-responsiveness translates to enhanced biological activity. Flow cytometry analysis revealed that cellular uptake of pRNLs was time-dependent and significantly higher at pH 6.5 compared to pH 7.4. At pH 6.5, the mean fluorescence intensity of cells treated with pRNLs was approximately 2.5-fold higher than that of nRNLs. This enhanced uptake is attributed to the de-PEGylation process, which removes the steric barrier and allows closer contact between the liposome and the cell membrane. Confocal laser scanning microscopy visually confirmed these findings, showing intense DOX fluorescence in the nuclei of cells treated with pRNLs at acidic pH, indicating successful endosomal escape and nuclear translocation of the drug.

Cytotoxicity assays provided a quantitative measure of therapeutic potential. Table 2 summarizes the IC50 values obtained from the MTT assays.

Table 2: IC50 Values (micromolar) of DOX Formulations against 4T1 Cells

Formulation	**pH 7.4 (48 hours)**	**pH 6.5 (48 hours)**
Free DOX	0.85 +/- 0.12	0.79 +/- 0.09
nRNLs	4.20 +/- 0.35	4.10 +/- 0.41
pRNLs	3.95 +/- 0.28	1.15 +/- 0.15

As indicated in Table 2, free DOX exhibited high toxicity regardless of pH due to its rapid diffusion mechanism. The nRNLs showed higher IC50 values (lower toxicity) at both pH levels, consistent with the "PEG dilemma" where stable liposomes are slowly internalized. However, the pRNLs demonstrated a dramatic decrease in IC50 at pH 6.5 (1.15 micromolar), approaching the potency of free DOX. This pH-dependent cytotoxicity confirms that the acidic environment triggers the activation of the nanocarrier, restoring the drug's availability. At pH 7.4, the higher IC50 of pRNLs suggests reduced toxicity towards normal tissues, a desirable characteristic for reducing side effects [14].

5. In Vivo Pharmacokinetics and Biodistribution

The pharmacokinetic profiles obtained from the animal studies highlighted the advantages of the liposomal formulations over free drug administration. Free DOX was rapidly cleared from the circulation with a very short half-life, consistent with its small molecular weight and susceptibility to renal clearance and metabolism. In contrast, both liposomal formulations exhibited significantly prolonged circulation times. The AUC (Area Under the Curve) for pRNLs was found to be approximately 15-fold higher than that of free DOX. Using the algorithms described in Code Listing 1, we calculated the Mean Residence Time (MRT) and elimination half-life. The MRT for pRNLs was comparable to nRNLs, indicating that the pH-sensitive modification did not compromise the stealth properties of the PEG layer under physiological conditions in the bloodstream. This stability is essential for the passive targeting mechanism, as long-circulating carriers have a higher probability of passing through the leaky vasculature

of the tumor. Biodistribution analysis at 24 hours post-injection provided critical insights into tissue accumulation. Free DOX showed high accumulation in the heart and kidneys, explaining its known cardiotoxicity and nephrotoxicity. The liposomal formulations significantly reduced accumulation in the heart. Notably, the pRNLs showed the highest accumulation in the tumor tissue, significantly surpassing nRNLs. This enhanced accumulation is likely a synergistic result of the EPR effect (facilitated by long circulation) and the pH-triggered retention within the tumor matrix. Once the pRNLs enter the acidic tumor interstitium, the loss of PEG and surface charge reversal may prevent the liposomes from washing back into the circulation, effectively trapping them in the tumor site [15].

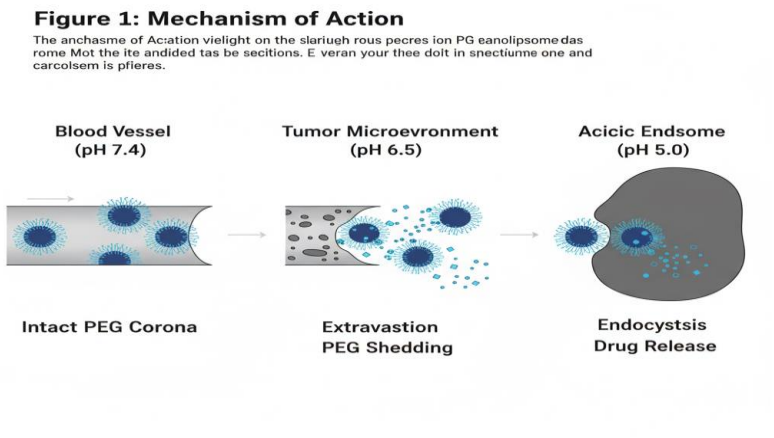

Figure 1: *Mechanism of Action*

6. In Vivo Antitumor Efficacy and Safety

The ultimate test of the nanocarrier's utility is its ability to inhibit tumor growth in a living organism. In the murine 4T1 breast cancer model, the saline control group showed rapid tumor progression, with tumor volumes exceeding 1500 cubic millimeters by day 21. Treatment with free DOX slowed tumor growth but was accompanied by significant body weight loss (greater than 15 percent), indicating severe systemic toxicity. The nRNLs showed moderate tumor inhibition, likely limited by poor cellular uptake. The pRNLs treatment group exhibited the most potent antitumor effect, with tumor growth inhibition rates significantly higher than both free DOX and nRNLs groups. The average tumor volume in the pRNLs group was maintained below 400 cubic millimeters at the end of the study. Importantly, the mice in the pRNLs group maintained steady body weight throughout the treatment period, suggesting a favorable safety profile. Survival analysis indicated that mice treated with pRNLs had a significantly extended lifespan compared to all other groups.

Histological evaluation using H&E staining further corroborated these findings. Tumor sections from the pRNLs group showed extensive areas of necrosis and apoptosis, indicating effective drug delivery and cytotoxic action. Conversely, heart tissue sections from the free DOX group displayed disarray of myocardial fibers and vacuolization, classic signs of anthracycline-induced cardiotoxicity. In sharp contrast, heart tissues from the pRNLs group appeared structurally normal, indistinguishable from the saline control. This protective effect is a direct consequence of the liposomal encapsulation and the stability of the carrier at physiological pH, which prevents high peak concentrations of free DOX in the myocardium. The liver and kidney sections of

the pRNLs group showed no significant signs of inflammation or damage, suggesting that the components of the liposome and the degradation products of the hydrazone linker are biocompatible and biodegradable. These results collectively demonstrate that the pH-responsive nanoliposome system not only enhances the therapeutic efficacy of DOX against breast cancer but also significantly ameliorates its dose-limiting side effects.

7. Conclusion

In this research, we successfully designed, characterized, and evaluated a pH-responsive DOX-loaded PEGylated nanoliposome system for targeted breast cancer therapy. The incorporation of a pH-labile hydrazone linkage allowed the nanocarrier to resolve the paradox between long circulation and efficient cellular uptake. Physicochemical characterization confirmed the formation of stable, uniform vesicles that respond to acidic stimuli by altering their surface properties and releasing their payload. In vitro studies validated the pH-dependent release and enhanced cytotoxicity in acidic environments mimicking the tumor niche. Most significantly, in vivo evaluations demonstrated that the pRNLs possess superior pharmacokinetic properties, enhanced tumor accumulation, and potent antitumor efficacy compared to conventional non-responsive liposomes and free drug. The concurrent reduction in cardiotoxicity highlights the clinical relevance of this approach. While further studies are required to optimize the lipid ratios and explore efficacy in metastatic models, the current findings establish the pH-responsive nanoliposome as a robust platform for the safe and effective delivery of chemotherapeutics in oncology. Future work will focus on the potential of co-delivering multiple agents and modifying the surface with active targeting ligands to further increase specificity.

References

Gupta, R., Yin, L., Grosche, A., Lin, S., Xu, X., Guo, J., ... & Vidyasagar, S. (2020). An amino acid–based oral rehydration solution regulates radiation-induced intestinal barrier disruption in mice. The Journal of nutrition, 150(5), 1100-1108.

Hadjidimitriou, S. K., & Hadjileontiadis, L. J. (2012). Toward an EEG-based recognition of music liking using time-frequency analysis. IEEE Transactions on Biomedical Engineering, 59(12), 3498-3510.

Higgins, J. P. (2002). Nonlinear systems in medicine. The Yale journal of biology and medicine, 75(5-6), 247.

Meng, L., Shan, T., Li, K., & Gong, Q. (2021). Long-term tract-specific white matter microstructural changes after acute stress. Brain imaging and behavior, 15(4), 1868-1875.

Harrington, J., & Yamamoto, S. (2026). Synergistic Effects of Combined Therapies for Gastrointestinal Disorders: Analysis via Response Surface Methodology. Computer Science Bulletin, 9(1), 96-102.

Shan, T., Cappelloni, M. S., & Maddox, R. K. (2024). Subcortical responses to music and speech are alike while cortical responses diverge. Scientific Reports, 14(1), 789.

Wang, Y. (2025, April). Efficient adverse event forecasting in clinical trials via transformer-augmented survival analysis. In Proceedings of the 2025 International Symposium on Bioinformatics and Computational Biology (pp. 92-97).

Wang, Y. (2025, August). AI-AugETM: An AI-augmented exposure–toxicity joint modeling framework for personalized dose optimization in early-phase clinical trials. In 2025 19th International Conference on Complex Medical Engineering (CME) (pp. 182-186). IEEE.

Ren, Y., Wu, D., & Lopez–De Fede, A. (2022, June). Identification and Prediction of Low-Birthweight Baby Outcomes and Mom Risk Factors. In 2022 IEEE 10th International Conference on Healthcare Informatics (ICHI) (pp. 01-02). IEEE.

Shan, T., Lalor, E. C., & Maddox, R. K. (2026). Chimeric music reveals an interaction of pitch and time in electrophysiological signatures of music encoding. Journal of Neuroscience, 46(4).

Smith, J., Anderson, R., & Miller, W. (2026). Predicting Efficacy of Immune Checkpoint Inhibitors in Targeted Oncology Therapy using Multi-Modal Deep Learning. Frontiers in Healthcare Technology, 3(1), 31-39.

Ren, Y., Wu, Y., Fan, J. W., Khurana, A., Fu, S., Wu, D., ... & Huang, M. (2024). Automatic uncovering of patient primary concerns in portal messages using a fusion framework of pretrained language models. Journal of the American Medical Informatics Association, 31(8), 1714-1724.

Wang, Y. (2025, June). RAGNet: Transformer–GNN–Enhanced Cox–Logistic Hybrid Model for Rheumatoid Arthritis Risk Prediction. In Proceedings of the 2025 International Conference on Health Informatization and Data Analytics (pp. 90-94).

Wu, J., Liu, L., Hu, J., Zhang, L., Jia, S., Wang, C., ... & Yu, D. (2025). The interaction between nanoscale MIL-53 (Fe) and Fzd6 protein drives enhanced bone regeneration. Materials & Design, 115248.

Saito, T., & Sasaki, K. (2026). Identification of Novel Circulating Biomarkers for Early Cancer Detection using High-Dimensional Feature Selection Algorithms. Multidisciplinary Research in Computing Information Systems, 6(1), 63-71.